The crystal chemistry of the amphiboles II
Refinement of the crystal structure of oxy-kaersutite

F. C. HAWTHORNE AND H. D. GRUNDY

Department of Geology, McMaster University, Hamilton, Ontario, Canada

SUMMARY. Three-dimensional counter-diffractometer data corrected for absorption and a full matrix least-squares method have been used to refine the crystal structure of an oxy-kaersutite in the space group $C2/m$. The chemical composition of the amphibole is $Na_{0.543}K_{0.434}Ca_{1.916}Mg_{3.188}Fe^{3+}_{1.064}$ $Ti_{0.515}Mn_{0.009}Al_{0.370}Si_{5.878}Al_{2.122}O_{22}(O^{2-})_2$ with cell parameters a 9·8920(11), b 18·064(2), c 5·3116(7)Å and β 105·388(5)°. Cation site occupancies were refined using bulk chemical constraints and the A-site positionally disordered. The final conventional R-factor for 1041 observed reflections is 4·0 %.

The rotation of the tetrahedral chains in calcic clino-amphiboles is shown to be a function of the Al^{iv} content of the tetrahedral sites. Comparison of this oxidized amphibole with an hydroxy-amphibole of similar chemical composition indicates that on oxidation the maximum amount of structural relaxation takes place in the vicinity of the $M(1)$ octahedra, which distort to a high-energy configuration.

KAERSUTITE is a titaniferous calcic amphibole, typically associated with alkaline igneous rocks in which it occurs as discrete phenocrysts or as a constituent of reaction rims. The ideal formula may be written:

$$Ca_2(Na,K)(Mg,Fe^{2+},Fe^{3+})_4Ti(Si_6Al_2)O_{22}(OH,F)_2;$$
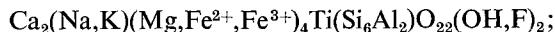
however, most naturally occurring species are somewhat deficient in Ti, which usually ranges from 0·5 to 1·0 atoms per formula unit. The substitution of $(Fe^{2+}+Fe^{3+})$ for Mg^{2+} rarely exceeds 1·5 atoms per formula unit and tetrahedral aluminium often exceeds the normal maximum of 2·0 atoms per formula unit. Recent site-refinements of Kakanui hornblende and potassium richterite (Brown and Gibbs, 1970, p. 1601) show that tetrahedral aluminium is completely ordered into the $T(1)$ tetrahedron. If this is the case in kaersutite, slight deviations from Lowenstein's rule (1954) must occur. The Fe^{2+}/Fe^{3+} ratio is low to moderate but can be zero in kaersutite from volcanic rocks, suggesting that oxidation occurs (in the crystalline state) on extrusion, giving oxy-kaersutite. Thus in volcanic rocks the Fe^{3+} may be expected to be distributed over all three octahedral sites ($M(1)$, $M(2)$, and $M(3)$) rather than ordered into the $M(2)$ site as is found in most normal amphiboles (Hawthorne and Grundy, 1973).

In this work the crystal structure of an oxy-kaersutite has been refined both to examine the tetrahedral chain configuration for the possibility of Al–O–Al linkages, and to characterize the octahedral distortions when small ions (Fe^{3+}) substitute into the $M(1)$ and $M(3)$ positions.

Experimental. The amphibole used in this study was from a phonolite collected in the Kangerdluarsuq area of Southern Greenland, and occurs as small phenocrysts in

an extremely fine-grained matrix. The crystals were removed with a needle, polished to remove any traces of the matrix and crushed to 100 mesh. The powder was examined under a microscope and found to be pure. This powder was then analyzed by wet chemical methods and the results are given in Table I.

TABLE I. *Crystal data for oxy-kaersutite from Kangerdluarsuq*†

		Atomic ratios‡			
SiO_2	39·90	Si	5·878		a 9·8920(11) Å
TiO_2	4·65	Al^{iv}	2·122		b 18·064(2) Å
Al_2O_3	14·35	Tetrahedral Σ	8·000		c 5·3116(7) Å
Fe_2O_3	9·60	Al^{vi}	0·370		β 105·388(5)°
FeO	0·04	Fe^{3+}	1·064		V 915·1(4) Å³
MnO	0·08	Fe^{2+}	—	Space group	$C2/m$
MgO	14·52	Mg	3·188	Z	2
CaO	12·14	Mn	0·009	$\mu(cm^{-1})$	24·5
Na_2O	1·90	Ti	0·515	Crystal size (mm)	0·040 × 0·095 × 0·230
K_2O	2·31	Octahedral Σ	5·146	Radiation/filter	Mo/Zr
H_2O^+	0·48	Ca	1·916	Crystal axis for data collection	[101]*
H_2O^-	0·02	Na	0·543		
F	0·12	K	0·434	No. of non-equivalent $\|F$rel$\| > 0$	1041
		Large cations	2·893	Final R (unit weights)	0·040
				Average $\hat{\sigma}$ $\|F\|$	2·60

† Analysis by John Muysson, Dept. of Geology, McMaster University, Hamilton, Canada.
‡ Calculation based on 24 (O, OH, F).

Single-crystal precession photographs show sharp diffraction maxima with no evidence of streaking or subsidiary maxima. The diffraction symmetry, $2/mC-/-$, is consistent with the space groups $C2$, Cm, and $C2/m$; as a result of a statistical test made on the data the centric space group $C2/m$ was chosen.

Unit cell dimensions were determined by a least-squares method using 31 carefully selected reflections measured manually on a GE-XRD6 semi-automatic single-crystal diffractometer, and are listed in Table I together with other information pertinent to this crystal. Data collection and reduction methods are identical to those reported by Hawthorne and Grundy (1973).

Refinement of the structure. The final atomic coordinates and temperature factors of ferrotschermakite (Hawthorne and Grundy, 1973) were used as initial parameters for the least-squares program.[1] Atomic scattering factors were taken from Doyle and Turner (1968), Tokonami (1965), and Cromer and Mann (1968).

One cycle of full matrix least-squares refinement varying the atomic positions[2] reduced the R-factor from 34 % to 18 % where $R = \Sigma|F_{obs} - F_{calc}|/\Sigma|F_{obs}|$.

[1] Where not stated, all computer programs used during data collection, reduction, and refinement are from *X-ray 67, Program System for X-ray Crystallography*, by J. M. Stewart, University of Maryland, adapted by H. D. Grundy for the CDC6400.
[2] Scaling of the observed data was accomplished through a scale factor that was included as a parameter in the refinement and allowed to vary at all times.

Site occupancies were then adjusted to agree with the chemical analysis (Table I) and varied for two cycles during which the R-factor dropped to 11 %. By varying the isotropic temperature factors with all else fixed, the R-factor was further reduced to 8 %. Numerous subsequent cycles of refinement varying the atomic positions, isotropic temperature factors, and site occupancies resulted in an R-factor of 7·3 %. On the basis of Fourier sections through the A-site (Hawthorne and Grundy, 1972) and the regular distributions of the peaks and troughs in the different Fourier sections, the

TABLE II. *Atom site positions and populations*

Site	x	y	z	B_{equiv}	Population
O(1)	0·1058(4)	0·0870(2)	0·2196(7)	0·76	1·00 O^{2-}
O(2)	0·1184(4)	0·1713(2)	0·7291(7)	0·75(5)	1·00 O^{2-}
O(3)	0·1065(5)	0	0·7160(10)	0·94(7)	1·00 O^{2-}
O(4)	0·3651(4)	0·2514(2)	0·7891(8)	0·86(5)	1·00 O^{2-}
O(5)	0·3504(4)	0·1402(2)	0·1107(7)	1·01(5)	1·00 O^{2-}
O(6)	0·3469(4)	0·1181(2)	0·6094(8)	1·02(5)	1·00 O^{2-}
O(7)	0·3414(6)	0	0·2859(12)	1·27(8)	1·00 O^{2-}
T(1)	0·2823(1)	0·08560(7)	0·3045(3)	0·47(2)	0·53(4)Si+0·47(4)Al
T(2)	0·2908(1)	0·17304(7)	0·8118(3)	0·48(2)	0·94(4)Si+0·06(4)Al
M(1)	0	0·08171(1)	1/2	0·66(4)	0·343(9)Fe^{3+}+0·657(9)Mg^{2+}
M(2)	0	0·1767(1)	0	0·63(4)	0·056(9)Fe^{3+}+0·502(9)Mg^{2+}+0·185Al^{3+}+0·257Ti
M(3)	0	0	0	0·64(6)	0·235(14)Fe^{3+}+0·765(14)Mg^{2+}
M(4)	0	0·27890(8)	1/2	0·84(3)	0·009Mn^{2+}+0·958Ca^{2+}+0·010(15)Fe^{3+}+0·025(15)Mg^{2+}
A(2)	0	0·4917(8)	0	1·15(5)	(Na_x+K_y)
A(m)	0·0467(11)	1/2	0·0901(22)	1·76(7)	$(Na_{0·543-x}+K_{0·434-y})$

$\left.\right\}x+1·8y = 0·802(10)$

A-site was positionally disordered both in the mirror plane and along the twofold axis. The starting parameters for the disordered A-site atoms were taken from Fourier maps. One cycle of least-squares refinement varying the atomic positions and occupancies of these disordered sites reduced the R-factor from 7·3 % to 5·4 % and the weighted R_w-factor from 7·6 % to 5·6 % where $R_w = [\Sigma w(F_{obs}-F_{calc})^2/\Sigma wF_{obs}^2]^{\frac{1}{2}}$ and $w = 1$. This improvement is significant at the 0·005 level (Hamilton, 1965). The temperature factors were then converted to anisotropic and several cycles of least-squares, gradually increasing the number of parameters varied, resulted in convergence at an R-value of 4·3 %.

At this stage these parameters were used as input to the least-squares program REFINE with which it is possible to apply chemical constraints during the least-squares fitting procedure (Finger, 1969a, b). Initial tetrahedral Al occupancies were assigned on mean bond length criteria (Papika *et al.*, 1969). Bulk chemical constraints were applied to the occupancies of all sites according to the chemical analysis; because the A-site is positionally disordered into the A(2) and A(m) sites, a chemical constraint cannot be applied in terms of Na^+ and K^+ but solely in terms of the number of electrons. The refinement converged[1] at an R-factor of 4·0 %. The final atomic positional parameters and equivalent isotropic temperature factors are presented in Table II. Interatomic distances and angles were calculated using the program ERRORS in which the errors are calculated using the full variance-covariance matrix (Finger,

[1] Tables of F_{obs} and the final F_{calc} can be obtained from the authors or from the Dept. of Mineralogy, British Museum (Natural History), Cromwell Road, London S.W.7.

TABLE IIIa. *Interatomic distances in oxy-kaersutite*

Atoms	Bond multiplicity	Distance	Atoms	Bond multiplicity	Distance
	T(1) Tetrahedron			*T(2) Tetrahedron*	
$T(1)–O(1)$	1	1·684(4) Å	$T(2)–O(2)$	1	1·644(4) Å
$T(1)–O(5)$	1	1·689(4)	$T(2)–O(4)$	1	1·615(4)
$T(1)–O(6)$	1	1·682(5)	$T(2)–O(5)$	1	1·651(5)
$T(1)–O(7)$	1	1·665(2)	$T(2)–O(6)$	1	1·663(4)
Mean $T(1)–O$		1·680	Mean $T(2)–O$		1·643
	M(1) Octahedron			*M(3) Octahedron*	
$M(1)–O(1)$	2	2·037(5)	$M(3)–O(1)$	4	2·070(4)
$M(1)–O(2)$	2	2·173(5)	$M(3)–O(3)$	2	2·060(6)
$M(1)–O(3)$	2	1·988(5)	Mean $M(3)–O$		2·067
Mean $M(1)–O$		2·066			
	M(2) Octahedron			*M(4) Polyhedron*	
$M(2)–O(1)$	2	2·106(5)	$M(4)–O(2)$	2	2·424(5)
$M(2)–O(2)$	2	2·085(5)	$M(4)–O(4)$	2	2·351(5)
$M(2)–O(4)$	2	1·981(5)	$M(4)–O(5)$	2	2·642(6)
Mean $M(2)–O$		2·057	$M(4)–O(6)$	2	2·560(4)
			Mean $M(4)–O$		2·494
	A(m) Polyhedron			*A(2) Polyhedron*	
A(m) O(5)	2	3·026(6)	A(2)–O(5)	2	2·945(11)
A(m)–O(5)	2	3·210(7)	A(2)–O(5)	2	3·192(12)
A(m)–O(6)	2	2·705(8)	A(2)–O(6)	2	2·978(11)
A(m)–O(6)	2	3·507(11)	A(2)–O(6)	2	3·185(12)
A(m)–O(7)	1	2·515(11)	A(2)–O(7)	2	2·460(7)
A(m)–O(7)	1	2·527(11)	A(2)–O(7)	2	3·703(9)
A(m)–O(7)	1	3·204(12)	Mean for 12		3·078
A(m)–O(7)	1	4·104(12)	Mean for 8		2·893
Mean for 12		3·104			
Mean for 8		2·866			
	Conventional A site			*M–M*	
A–O(5)	4	3·068(4)	$M(1)–M(1)$		2·950(4)
A O(6)	4	3·079(3)	$M(1)–M(2)$		3·163(1)
A–O(7)	2	2·456(4)	$M(1)–M(3)$		3·038(1)
A–O(7)	2	3·700(4)	$M(1)–M(4)$		3·563(3)
Mean for 12		3·075	$M(2)–M(3)$		3·192(2)
			$M(2)–M(4)$		3·234(1)
	A–T				
A(m)–T(1)		3·395(9)		*Miscellaneous*	
A(m)–T(2)		3·490(5)	A(m)–A(m′)		1·140(11)
A(2)–T(1)		3·324(7)	A(2)–A(2′)		0·299(29)
A(2) T(2)		3·611(7)	A(m)–A(2)		0·589(11)
	$T(1)–T(2)$				
$T(1)–T(2)$ [through O(6)]		3·106(2)			
$T(1)–T(2)$ [through O(5)]		3·077(2)			
$T(1)–T(1)$ [across mirror]		3·091(3)			

TABLE III*b*. *Oxygen–oxygen polyhedral edge lengths*

Atoms*	Distance	Atoms	Distance
T(1) Tetrahedron		*T*(2) Tetrahedron	
O(1)–O(5)	2·803(5) Å	O(2)–O(4)	2·782(5) Å
O(1)–O(6)	2·770(9)	O(2)–O(5)	2·688(9)
O(1)–O(7)	2·755(6)	O(2)–O(6)	2·683(5)
O(5)–O(6)	2·688(6)	O(4)–O(5)	2·667(5)
O(5)–O(7)	2·707(4)	O(4)–O(6)	2·579(5)
O(6)–O(7)	2·731(5)	O(5)–O(6)	2·684(6)
Mean O–O	2·742	Mean O–O	2·680
M(1) Octahedron		*M*(3) Octahedron	
O(1^u)–O(2^d)	2·764(5)	O(1^u)–O(1^d)	2·689(10)
O(1^u)–O(2^u)	3·079(6)	O(1^u)–O(1^u)	3·142(7)
O(1^u)–O(3^d)	2·718(5)	O(1^u)–O(3^d)	2·718(5)
O(1^u)–O(3^u)	3·064(6)	O(1^u)–O(3^u)	3·107(6)
O(2)–O(2)	2·896(10)	Mean O–O	2·914
O(2)–O(3)	3·097(4)		
O(3)–O(3)	2·666(13)	*M*(4) Polyhedron	
Mean O–O	2·917	O(2)–O(2)	2·896(10)
		O(2^u)–O(4^u)	3·128(5)
M(2) Octahedron		O(2^u)–O(4^d)	2·958(5)
O(1)–O(1)	2·689(10)	O(2^u)–O(5^u)	3·504(5)
O(1^u)–O(2^d)	2·764(5)	O(4^u)–O(5^d)	3·383(6)
O(1^u)–O(2^u)	3·049(6)	O(4^u)–O(6^u)	2·579(5)
O(1)–O(4)	2·935(5)	O(5^u)–O(6^u)	2·688(6)
O(2^u)–O(4^d)	2·958(5)	O(5^u)–O(6^d)	2·994(8)
O(2^u)–O(4^u)	2·881(5)	O(6^u)–O(6^d)	3·519(8)
O(4)–O(4)	2·994(11)	Mean O–O	3·055
Mean O–O	2·905		

* The superscript notation refers to oxygen x coordinate greater (u) or less (d) than the x coordinate of M.

personal communication); these are shown in Tables III and IV respectively. The temperature factor form used was

$$\exp\left[-\sum_{i=1}^{3}\sum_{j=1}^{3} h_i\, h_j\, \beta_{ij}\right],$$

and the β_{ij} are given in Table V. The magnitudes and orientations of the principal axes of the thermal ellipsoids were calculated and are presented in Table VI. The values shown in these tables are physically realistic and are very similar to those of other calcic amphiboles, which have been discussed elsewhere (Papike *et al.*, 1969) and therefore will not be considered any further in this paper.

Discussion[1]

Tetrahedral cation sites. As in the case of the Kakanui hornblende and the K-richterite (Papike *et al.*, 1969), the tetrahedral aluminium of the oxy-kaersutite is

[1] Fig. 1 illustrates the basic structure of kaersutite and the atomic nomenclature used in this discussion.

TABLE IV. *Selected interatomic angles*

Atoms	Angle	Atoms	Angle
T(1) *Tetrahedron*		*T*(2) *Tetrahedron*	
O(1)–*T*(1)–O(5)	112·4(2)°	O(2)–*T*(2)–O(4)	117·2(2)°
O(1)–*T*(1)–O(6)	110·8(3)	O(2)–*T*(2)–O(5)	109·3(3)
O(1)–*T*(1)–O(7)	110·7(2)	O(2)–*T*(2)–O(6)	108·5(2)
O(5)–*T*(1)–O(6)	105·8(2)	O(4)–*T*(2)–O(5)	109·5(2)
O(5)–*T*(1)–O(7)	107·6(3)	O(4)–*T*(2)–O(6)	103·8(2)
O(6)–*T*(1)–O(7)	109·4(3)	O(5)–*T*(2)–O(6)	108·2(2)
Mean O–*T*(1)–O	109·5	Mean O–*T*(2)–O	109·4
M(1) *Octahedron*		*M*(3) *Octahedron*	
O(1ᵘ)–*M*(1)–O(2ᵈ)	82·0(1)	O(1ᵘ)–*M*(3)–O(1ᵈ)	81·1(3)
O(1ᵘ)–*M*(1)–O(2ᵘ)	94·0(1)	O(1ᵘ)–*M*(3)–O(1ᵘ)	98·9(3)
O(1ᵘ)–*M*(1)–O(3ᵈ)	84·9(2)	O(1ᵘ)–*M*(3)–O(3ᵈ)	82·3(1)
O(1ᵘ)–*M*(1)–O(3ᵘ)	99·1(2)	O(1ᵘ)–*M*(3)–O(3ᵘ)	97·7(1)
O(2)–*M*(1)–O(2)	83·6(2)	Mean O–*M*(3)–O	90·0
O(2)–*M*(1)–O(3)	96·1(2)		
O(3)–*M*(1)–O(3)	84·2(3)	*M*(4) *Polyhedron*	
Mean O–*M*(1)–O	90·0	O(2)–*M*(4)–O(2)	73·4(2)
		O(2ᵘ)–*M*(4)–O(4ᵈ)	76·6(1)
M(2) *Octahedron*		O(2ᵘ)–*M*(4)–O(4ᵘ)	81·9(1)
O(1)–*M*(2)–O(1)	79·4(3)	O(2ᵘ)–*M*(4)–O(5ᵘ)	87·4(2)
O(1ᵘ)–*M*(2)–O(2ᵈ)	82·5(1)	O(4ᵘ)–*M*(4)–O(5ᵈ)	85·1(1)
O(1ᵘ)–*M*(2)–O(2ᵘ)	93·4(1)	O(4ᵘ)–*M*(4)–O(6ᵘ)	63·2(1)
O(1)–*M*(2)–O(4)	91·7(2)	O(5ᵘ)–*M*(4)–O(6ᵈ)	70·3(2)
O(2ᵘ)–*M*(2)–O(4ᵈ)	93·3(2)	O(5ᵘ)–*M*(4)–O(6ᵘ)	62·2(1)
O(2ᵘ)–*M*(2)–O(4ᵘ)	90·2(1)	O(6)–*M*(4)–O(6)	86·8(2)
O(4)–*M*(2)–O(4)	98·2(3)	Mean O–*M*(4)–O	75·9
Mean O–*M*(2)–O	90·0		
		Tetrahedral Chain	
*A Polyhedron**		*T*(1)–O(5)–*T*(2)	134·3(3)
O(7)–O(7)–O(7)	64·5(1)	*T*(1)–O(6)–*T*(2)	136·4(2)
Δ = 0·283		*T*(1)–O(7)–*T*(1)	136·4(3)
		O(5)–O(6)–O(5)	162·9(2)
		O(5)–O(7)–O(6)	161·8(2)

* Δ = {90° − [O(7)–O(7)–O(7)]}/90°.

strongly ordered into $T(1)$, which is the larger of the two tetrahedral cation sites. However, both site refinement and bond length criteria (Papike *et al.*, 1969; Hawthorne and Grundy, 1973) indicate that sufficient Al^{3+} occurs in $T(2)$ to avoid any Al–O–Al linkages across the O(7). Thus Lowenstein's Al avoidance rule (Lowenstein, 1954) need not be violated in this particular amphibole. A similar result has also been obtained by the refinement of an aluminous hastingsite containing 2·73 tetrahedral Al^{3+} ions per formula unit (in progress).

In the clinoamphiboles the amount of kinking in the tetrahedral chain is indicated by the O(5)–O(6)–O(5) angle. Fig. 2 is a plot of this angle against tetrahedral aluminium content for the Ca-rich clinoamphiboles. It is apparent that the substitution of the larger Al^{3+} ion for Si^{4+} in the tetrahedral chain results in a systematic decrease in the

O(5)–O(6)–O(5) angle (i.e. increased kinking) as each individual of the chain rotates to offset its increase in size. In particular this rotation results in a decrease in the b and c dimensions of the chain in order to match them with the b and c dimensions of the octahedral strip.

Octahedral cation sites. Cations were assigned to sites on the basis of crystal chemical criteria. Due to its relatively large ionic radius all Ca^{2+} was placed in $M(4)$ where the mean metal–oxygen distance is significantly larger than those of the octahedral sites

TABLE V. *Temperature factor coefficients for oxy-kaersutite*

| Atom	B_{ISO} or $\beta_{11}(\hat{\sigma})$	$\beta_{22}(\hat{\sigma})$	$\beta_{33}(\hat{\sigma})$	$\beta_{12}(\hat{\sigma})$	$\beta_{13}(\hat{\sigma})$	$\beta_{23}(\hat{\sigma})$
$T(1)$	0·00166(13)	0·00029(3)	0·00433(44)	−0·00011(5)	0·00080(19)	−0·00007(9)
$T(2)$	0·00143(12)	0·00032(3)	0·00480(42)	−0·00005(5)	0·00057(18)	0·00005(9)
$M(1)$	0·00211(18)	0·00035(6)	0·00697(66)	0	0·00169(25)	0
$M(2)$	0·00194(19)	0·00038(5)	0·00727(69)	0	0·00159(26)	0
$M(3)$	0·00234(29)	0·00027(7)	0·00619(102)	0	0·00057(39)	0
$M(4)$	0·00309(15)	0·00055(4)	0·00896(55)	0	0·00362(22)	0
$O(1)$	0·00222(34)	0·00058(9)	0·00719(126)	−0·00014(14)	0·00138(52)	−0·00020(27)
$O(2)$	0·00191(30)	0·00061(9)	0·00784(117)	0·00013(14)	0·00153(47)	0·00031(27)
$O(3)$	0·00282(52)	0·00060(13)	0·00994(81)	0	0·00153(80)	0
$O(4)$	0·00333(36)	0·00043(9)	0·00832(135)	−0·00015(15)	0·00211(57)	0·00014(29)
$O(5)$	0·00303(36)	0·00085(9)	0·00784(121)	−0·00008(15)	0·00124(53)	0·00103(30)
$O(6)$	0·00282(36)	0·00077(9)	0·01104(135)	0·00008(15)	0·00244(56)	−0·00110(31)
$O(7)$	0·00268(54)	0·00063(14)	0·01804(227)	0	0·00010(90)	0
$A(m)$	1·76(13)					
$A(2)$	1·15(15)					

(see Table III*a*). The small amount of Mn^{2+} was also assigned to $M(4)$ on the basis of site preference shown by refinement of the structure of Mn-cummingtonite (Papike *et al.*, 1969; Hawthorne and Grundy, in progress). Previous refinements of normal hydroxy-amphiboles (Papike and Clarke, 1968; Hawthorne and Grundy, 1973) indicate that the trivalent ions show a strong site-preference for the $M(2)$ octahedron; this is to be expected because of the highly underbonded nature of O(4). Consequently all the Al^{3+} and Ti was assigned to $M(2)$. In tremolite, where all the octahedral sites contain just one type of ion, the mean $M(2)$ metal–oxygen distance is greater than those of the $M(1)$ and $M(3)$ sites. In oxy-kaersutite the mean $M(2)$–O distance is less than the mean $M(1)$–O and $M(3)$–O distances indicating that the $M(2)$ site contains the smaller, more highly-charged ions. Because of the oxidized nature of this amphibole, it seems likely that most of the iron was ferrous on formation of the crystal and therefore, would probably be located in the $M(1)$ and $M(3)$ sites. This is borne out by the site-refinement of ferric iron. The bulk of the Fe^{3+} is in the $M(1)$ and $M(3)$ sites; the amount of Fe^{3+} in $M(4)$ is zero to within one standard deviation, and the amount in $M(2)$ is low. Possibly the iron in $M(2)$ was originally trivalent; certainly any iron in $M(2)$ will be far less susceptible to oxidation during dehydroxylation than the iron in $M(1)$ and $M(3)$, as $M(2)$ is not coordinated by the hydroxyl group as are the other two sites. $M(1)$ is enriched in Fe^{3+} relative to $M(3)$, and both are enriched relative to $M(2)$.

TABLE VI. *Ellipsoids of vibration*

Atom	R.M.S. displacement	Angle to a-axis	Angle to b-axis	Angle to c-axis
$T(1)$	0·067(4) Å²	75(9)°	17(8)°	87(21)°
	0·075(4)	74(12)	87(20)	177(21)
	0·089(4)	22(9)	107(7)	91(11)
$T(2)$	0·071(4)	72(15)	19(12)	101(19)
	0·079(4)	116(28)	88(23)	138(28)
	0·084(3)	147(25)	71(12)	50(28)
$M(1)$	0·076(6)	90	0	90
	0·095(4)	43(15)	90	148(15)
	0·107	47(15)	90	58(15)
$M(2)$	0·079(5)	90	0	90
	0·085(5)	31(11)	90	136(11)
	0·103(5)	59(11)	90	46(11)
$M(3)$	0·067(9)	90	0	90
	0·090(8)	103(14)	90	151(14)
	0·108(6)	13(14)	90	119(14)
$M(4)$	0·074(4)	136(2)	90	31(2)
	0·094(3)	90	0	90
	0·132(3)	47(2)	90	58(2)
$O(1)$	0·093(8)	81(242)	39(147)	56(277)
	0·094(8)	39(75)	73(252)	138(255)
	0·107(8)	52(26)	124(24)	68(26)
$O(2)$	0·088(8)	18(20)	98(49)	122(43)
	0·094(8)	94(59)	39(23)	126(42)
	0·110(7)	72(15)	52(19)	52(18)
$O(3)$	0·099(10)	90	0	90
	0·112(10)	25(136)	90	130(136)
	0·115(10)	65(136)	90	40(136)
$O(4)$	0·081(9)	105(10)	158(18)	70(19)
	0·101(9)	69(15)	111(19)	158(18)
	0·126(7)	27(13)	97(9)	80(14)
$O(5)$	0·082(9)	102(9)	126(7)	36(7)
	0·117(7)	154(17)	102(16)	98(13)
	0·134(7)	113(18)	39(8)	55(7)
$O(6)$	0·077(10)	116(9)	46(7)	48(6)
	0·120(7)	154(9)	112(14)	88(15)
	0·136(7)	86(17)	128(10)	42(6)
$O(7)$	0·102(11)	90	0	90
	0·111(11)	160(9)	90	94(9)
	0·160(10)	110(9)	90	4(9)

The angular distortions in the octahedral strip of oxy-kaersutite are similar to those seen in other calcic clinoamphiboles; all are apparently due to cation–cation repulsion across the shared edges with the exception of those also influenced by the necessary articulation requirements in the cross linkage of the octahedral and tetrahedral elements of the structure.

The distortion of an individual octahedral site may be estimated by the deviations of the cation–anion distances within the octahedron from their mean. It is profitable to examine the distortions of the $M(1)$, $M(2)$, and $M(3)$ octahedra in oxy-kaersutite with respect to those in Kakanui hornblende, which has a very similar chemical
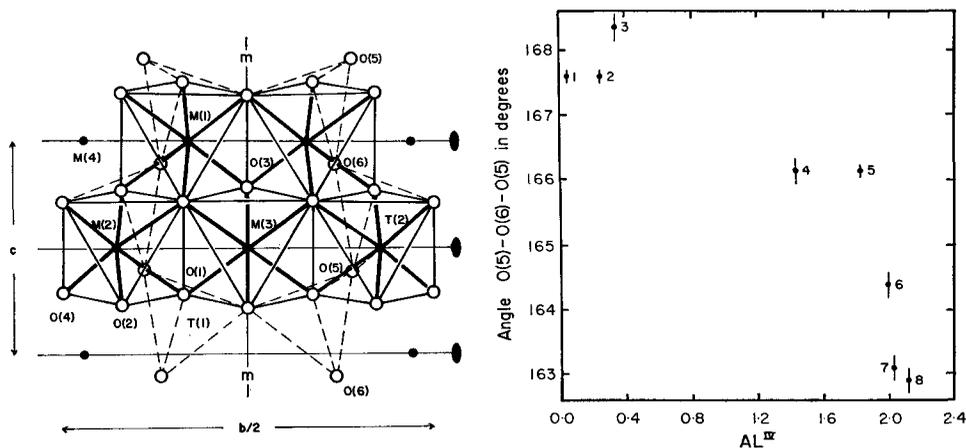
FIGS. 1 and 2: FIG. 1 (left). Diagram of oxy-kaersutite viewed along the normal to (100) showing selected portions of cell content. FIG. 2 (right). Plot of angle O(5)–O(6)–O(5) against tetrahedral aluminium content for the following Ca-rich clino-amphiboles: 1. Tremolite (Papike *et al.*, 1969). 2. Tremolite, x-ray and neutron data (Hawthorne and Grundy, in preparation). 3. Actinolite (Mitchell, Bloss, and Gibbs, 1971). 4. Barkevikite (unpublished data). 5. Ferrohastingsite (unpublished data). 6. Ferrotschermakite (Hawthorne and Grundy, 1973). 7. Kakanui hornblende (Papike *et al.*, 1969). 8. Oxy-kaersutite (this study).

TABLE VII. *Bond distances in oxy-kaersutite and Kakanui hornblende*

Atoms	Kakanui hornblende (Papike *et al.*, 1969)		Oxy-kaersutite (this study)	
	Bond distance	Δ*	Bond distance	Δ
$T(1)$–O(1)	1·667(4) Å	−0·002 Å	1·684(4) Å	+0·004 Å
–O(5)	1·678(5)	+0·009	1·689(4)	+0·009
–O(6)	1·670(5)	+0·001	1·682(5)	+0·002
–O(7)	1·660(3)	−0·009	1·665(2)	−0·015
Mean $T(1)$–O	1·669		1·680	
$T(2)$–O(2)	1·641(4)	+0·001	1·644(4)	+0·001
–O(4)	1·606(5)	−0·034	1·615(4)	−0·028
–O(5)	1·650(5)	+0·010	1·651(5)	+0·008
–O(6)	1·661(5)	+0·021	1·663(4)	+0·023
Mean $T(2)$–O	1·640		1·643	
$M(1)$–O(1)	2·042(5)	−0·033	2·037(5)	−0·029
–O(2)	2·141(4)	+0·066	2·173(5)	+0·107
–O(3)	2·043(4)	−0·032	1·988(5)	−0·078
Mean $M(1)$–O	2·075		2·066	
$M(2)$–O(1)	2·101(4)	+0·052	2·106(5)	+0·049
–O(2)	2·072(5)	+0·023	2·085(5)	+0·028
–O(4)	1·973(4)	−0·076	1·981(5)	−0·076
Mean $M(2)$–O	2·049		2·057	
$M(3)$–O(1)	2·083(4)	+0·002	2·070(4)	+0·003
–O(3)	2·076(7)	−0·005	2·060(6)	−0·007
Mean $M(3)$–O	2·081		2·067	

* Δ = (individuals bond distance)−(mean bond distance).

composition (Table VII). The distortions shown by the $M(2)$ and $M(3)$ octahedra are almost the same for both structures, whereas a comparison of the $M(1)$ octahedra shows marked differences.

The increased distortion of the $M(1)$ octahedron in oxy-kaersutite relative to Kakanui hornblende may be explained by a qualitative analysis of the dehydroxylation process that has occurred in this amphibole. For iron-rich amphiboles the oxidation reaction may be written (Ernst and Wai, 1970) as $Fe^{2+}-O-H \rightarrow Fe^{3+}-O+1/2H_2\uparrow$. This reaction will produce a bond valence deficiency on the $O(3)$ anion and a bond valence excess on the $O(1)$ and $O(2)$ anions unless a readjustment in the positions of the neighbouring atoms takes place. In particular the $M(1)-O(3)$ distance has to be reduced in order to maintain local electrostatic neutrality.

The atoms involved in this reduction are the oxygen atoms at the $O(3)^u$ and $O(3)^d$ sites on the shared edge joining the $M(1)$ octahedra and the cations on the $M(1)$ sites that oppose each other across this edge. Because of the site symmetry of the atoms involved there are only two ways in which the atomic rearrangement may be made: shortening of the $M(1)-M(1)$ distance along the twofold axis; or shortening of the $O(3)-O(3)$ shared edge within the mirror plane. The first way implies that the separation of the $O(3)^u-O(3)^d$ sites remains as in the Kakanui hornblende and that in order to obtain an $M(1)-O(3)$ distance of 1.988 Å characteristic of oxy-kaersutite the $M(1)-M(1)$ distance has to decrease from 3.103 Å to 2.956 Å. In contrast the second way implies that the $M(1)-M(1)$ separation remains constrained and that the $O(3)^u-O(3)^d$ distance decreases from 2.658 Å to 2.468 Å. From the values of $M(1)-O(3)$ 1.988 Å, $O(3)^u-O(3)^d$ $2.666(13)$ Å, and $M(1)-M(1)$ $2.950(4)$ Å observed in oxy-kaersutite it is clear that the major adjustment is a shortening of the $M(1)-M(1)$ distance and that the adjustment due to the second way is insignificant.

From a simple electrostatic viewpoint the increased charge on the $M(1)$ site due to oxidation of iron should result in an increased cation–cation repulsion across the shared $O(3^u)-O(3^d)$ octahedral edge. This effect is not apparent as the $M(1)-M(1)$ distance in oxy-kaersutite is substantially decreased rather than increased relative to that in the Kakanui hornblende. The $O(3^u)-O(3^d)$ shared edge of the $M(1)$ octahedra is the shortest octahedral edge in the hydroxyl amphiboles. This may be attributed to the high electronegativity of hydrogen, which, through the withdrawal of charge from the $O(3)$ oxygen to which it is coordinated, tends to reduce the repulsive forces in the $O(3^u)-O(3^d)$ octahedral edge. It may be expected therefore that the removal of hydrogen from an hydroxy-amphibole would result in an increased anion–anion repulsion and a corresponding expansion of this edge. This is not the case as the $O(3)^u-O(3)^d$ edge in oxy-kaersutite is almost identical to that in the Kakanui hornblende. As there is no increase in size it may be assumed that the shielding properties of this edge with regard to the neighbouring $M(1)$ cations will improve and consequently allow a much greater contraction in the $M(1)-M(1)$ separation than would otherwise occur. Obviously factors of quite local nature are involved in the attainment of electrostatic neutrality during the dehydroxylation, a decrease in the $M(1)-M(1)$ distance being preferred over any substantial shortening of the $O(3^u)-O(3^d)$ octahedral edge; this must therefore be energetically more favourable.

Conclusion. Two main conclusions may be drawn from the above work. Firstly, the substitution of Al^{3+} for Si^{4+} into the tetrahedral chain of the Ca-rich clino-amphiboles results in an increased kinking of the chain and is due to linking the relatively flexible but enlarged double chain to a much more rigid octahedral strip. Secondly, the bulk of the structural relaxation takes place in the $M(1)$ octahedra during the dehydoxylation of kaersutite and gives an equilibrium configuration of higher energy than that occurring in the hydroxy-amphiboles. This is the direct result of bond valence requirements versus cation–cation and anion–anion repulsive forces.

REFERENCES

BROWN (G. E.) and GIBBS (G. V.), 1970. *Amer. Min.* **55**, 1587–1607.
CLARK (J. R.), APPLEMAN (D. E.), and PAPIKE (J. J.), 1969. *Min. Soc. Amer. Spec. Paper* **2**, 31–5.
CROMER (D. T.) and MANN (J. B.), 1968. *Acta Cryst.* **A24**, 321–4.
DOYLE (P. A.) and TURNER (P. S.), 1968. Ibid. 390–7.
ERNST (W. G.) and WAI (C. M.), 1970. *Amer. Min.* **55**, 1226–58.
FINGER (L. W.), 1969a. *Carnegie Inst. Wash. Year Book* **67**, 216–17.
—— 1969b. *Min. Soc. Amer. Spec. Paper* **2**, 95–100.
HAWTHORNE (F. C.) and GRUNDY (H. D.), 1972. *Nature*, **235**, 72–3.
—— —— 1973. *Min. Mag.* **39**, 36–48.
HAMILTON (W. C.), 1965. *Acta Cryst.* **18**, 502–10.
LOWENSTEIN (W.), 1954. *Amer. Min.* **39**, 92–6.
MITCHELL (J. T.), BLOSS (F. D.), and GIBBS (G. V.), 1971. *Zeits. Krist.* **133**, 273–300.
PAPIKE (J. J.) and CLARK (J. R.), 1968. *Amer. Min.* **53**, 1156–73.
—— ROSS (M.), and CLARK (J. R.), 1969. *Min. Soc. Amer. Spec. Paper* **2**, 117–36.
TOKONAMI (M.), 1965. *Acta Cryst.* **A19**, 486.